[(η^5-C_5Me_5)Fe($Ph_2PCH_2CH_2CH_2PPh_2$)][SO_3CF_3], a Stable 16-Electron Complex with a Coordinating Counteranion and without Agostic Interaction: The Dramatic Role of a Trivial Methylene Group

Gilles Argouarch,† Paul Hamon,† Loïc Toupet,‡ Jean-René Hamon,† and Claude Lapinte*,†

Organométalliques et Catalyse: Chimie et Electrochimie Moléculaires, UMR CNRS 6509, Institut de Chimie de Rennes, and Groupe Matière Condensée et Matériaux, UMR 6626, Université de Rennes 1, Campus de Beaulieu, 35042 Rennes Cedex, France

Received September 13, 2001

The iron chloro complex Cp*(dppp)FeCl (Cp* = pentamethylcyclopentadienyl, dppp = 1,3-bis(diphenylphosphino)propane; **2**) was prepared from $FeCl_2$(dppp) and Cp*Li in 85% yield. The air-stable compound **2** was characterized by IR-FT, ^{1}H, ^{31}P, and ^{13}C NMR, cyclic voltammetry (CV), and X-ray crystal analysis. The experimental data indicate that this complex possesses the same electronic properties as its homologue Cp*(dppe)FeCl (dppe = 1,2-bis(diphenylphosphino)ethane; **2′**), but shorter distances between the chlorine atom and the hydrogen atoms of the dppp ligand give rise to through-space interactions. The hydride **3** was obtained by treatment of the chloro derivative **2** with $LiAlH_4$ (95%). The changes in the Fe−H bond stretching and redox potential induced by replacement of dppe by dppp is in agreement with the existence of two conformers for the iron hydrides **3** and **3′**. The 16-electron species [Cp*(dppp)Fe][OSO_2CF_3] (**4[OTf]**) is obtained by treatment of **3** with methyl triflate in diethyl ether (82%). The pseudo-C_{2v} conformation of **4[OTf]** is established by an X-ray analysis. Complex **4[OTf]** possesses a triplet ground state, as shown by the magnetic susceptibility measurements, ^{1}H NMR, and Mössbauer spectroscopy. The UV−vis data obtained for **4[OTf]** and its homologue **4′[PF_6]** suggest that the increase of the bite angle of the bis-phosphine should produce a decrease of the HOMO−LUMO gap of the triplet ground state with a pseudo-C_{2v} symmetry.

Introduction

The chemistry of the sterically crowded and electron-rich Cp*(dppe)Fe auxiliary is particularly rich. Indeed, this unit is stable as five-coordinate iron complexes[1] and accommodates six- and seven-coordinate derivatives, which were isolated as iron(0),[2] iron(I),[1] iron(II), iron(III), and iron(IV) complexes with a number of valence electrons ranging from 16 to 19.[2−5] This iron building block has also shown very attractive features for the elaboration of organometallic molecular wires.[6,7] Among all the properties of this iron fragment, its ability to provide 18-electron paramagnetic complexes, namely [Cp*(dppe)Fe($OCMe_2$)][SO_3CF_3][8] and [Cp*(dppe)Fe(OSO_2CF_3)],[1] remains among the most surprising feature of this family of compounds and recent DFT calculations could not explain such an intriguing feature.[9]

The unique behavior of the Cp*(dppe)Fe fragment results from a subtle balance of the steric, electronic, and geometric environment of the iron center provided by the Cp* and dppe ligands. In particular, the dppe, as all chelates, possesses three major characteristics: electron-donating ability, steric properties, and a rigid P−M−P angle often called "bite angle". In this paper we investigate the effect of the bite angle of the dppp ligand by substituting dppe by dppp. We focus our effort in the determination of the modification of the steric and electronic properties of the iron(II) complexes induced by the introduction of an extra methylene fragment between the two phosphorus atoms of the bidentate phosphine. We report here (i) the synthesis of the entry Cp*(dppp)FeCl compound (**2**) and its X-ray

* To whom correspondence should be addressed. E-mail: lapinte@univ-rennes1.fr.
† Organométalliques et Catalyse: Chimie et Electrochimie Moléculaires.
‡ Groupe Matière Condensée et Matériaux.

(1) Hamon, P.; Toupet, L.; Hamon, J.-R.; Lapinte, C. *Organometallics* **1996**, *15*, 10−12.
(2) Hamon, P.; Hamon, J.-R.; Lapinte, C. *J. Chem. Soc., Chem. Commun.* **1992**, 1602−1603.
(3) Roger, C.; Hamon, P.; Toupet, L.; Rabaâ, H.; Saillard, J.-Y.; Hamon, J.-R.; Lapinte, C. *Organometallics* **1991**, *10*, 1045−1054.
(4) Hamon, P.; Toupet, L.; Hamon, J.-R.; Lapinte, C. *Organometallics* **1992**, *11*, 1429−1431.
(5) (a) Thépot, J.-Y.; Guerchais, V.; Lapinte, C.; Toupet, L. *Organometallics* **1993**, *12*, 4843−4853. (b) Denis, R.; Toupet, L.; Paul, F.; Lapinte, C. *Organometallics* **2000**, *19*, 4240−4251.
(6) (a) Paul, F.; Lapinte, C. *Coord. Chem. Rev.* **1998**, *178−180*, 427−505. (b) Le Narvor, N.; Toupet, L.; Lapinte, C. *J. Am. Chem. Soc.* **1995**, *117*, 7129−7138. (c) Coat, F.; Lapinte, C. *Organometallics* **1996**, *15*, 477−480. (d) Guillemot, M.; Toupet, L.; Lapinte, C. *Organometallics* **1998**, *17*, 1928−1930.
(7) Paul, F.; Meyer, W. E.; Toupet, L.; Jiao, H.; Gladysz, J. A.; Lapinte, C. *J. Am. Chem. Soc.* **2000**, *122*, 9405−9414.
(8) Hamon, P.; Toupet, L.; Hamon, J.-R.; Lapinte, C. *J. Chem. Soc., Chem. Commun.* **1994**, 931−932.
(9) Costuas, K.; Saillard, J.-Y. *Organometallics* **1999**, *18*, 2505−2512.

10.1021/om0108245 CCC: $22.00
Publication on Web 03/07/2002

Scheme 1

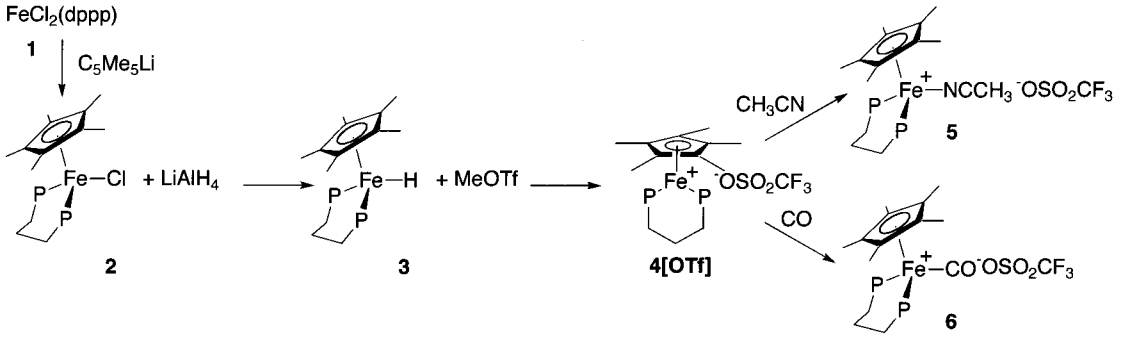

characterization which reveals the steric modification around the iron center, (ii) the conversion of **2** into the hydride Cp*(dppp)FeH complex (**3**), which presents an unexpected change in the Fe−H bonding as shown by IR-FT spectroscopy, (iii) the synthesis and the X-ray analysis of the 16-electron species [Cp*(dppp)Fe][SO_3CF_3] (**4[OTf]**), which coordinates neither the triflate anion nor the acetone, (iv) a full spectroscopic characterization of the paramagnetic complex **4**, including UV−vis spectroscopy, which demonstrates that the HOMO−LUMO gap in the 16-electron species decreases when the P−Fe−P angle increases, and (v) the basic reactivity of the coordinatively unsaturated complex **4-[OTf]**. Comparison between the compounds **2**, **3**, **4-[OTf]**, **5**, and **6** and their homologues of the dppe series, denoted **2′**, **3′**, **4′[PF$_6$]**, **5′**, and **6′**, respectively, evidences the role of the bite angle of the diphosphine in the properties of these iron complexes.

Results and Discussion

1. Synthesis and Characterization of Cp*(dppp)-FeCl (2). As outlined in Scheme 1, the iron chloro complex **2** was synthesized via a protocol similar to the one developed for the related Cp*(dppe)FeCl (**2′**) previously described.[3] The complex (dppp)$FeCl_2$ (**1**), which is air stable as a solid for extended periods, was reacted with Cp*Li in THF at 20 °C. Workup gave **2** as analytically pure black microcrystals in 85% yield. The ^{1}H chemical shifts of complex **2** are very similar to those of the related compound **2′** of the dppe series[3] (see Experimental Section). However, we note that the introduction of an extra methylene group in the alkyl chain which links the two phosphorus atoms of the dppp ligand produces a downfield shift of the ^{31}P resonance from δ 91.6 (observed for **2′**) to δ 50.9. Moreover, whereas the ^{1}H resonance for the methylene protons of the complex **2′** are observed in the range δ 1.50−2.00, a signal corresponding to two protons is observed at δ 2.54 ppm in the case of complex **2**. This upfield shift could be due to 1,3-diaxial interactions between hydrogen atoms of the methylene groups bound to the phosphorus atoms and the chlorine (see below). In the limit of the accuracy of the cyclic voltammetry measurement, both complexes **2** and **2′** possess the same reversible one-electron-oxidation potential (Table 1).

2. X-ray Crystal Structure of 2. Monocrystals of **2** were grown by slow diffusion of pentane in a concentrated CH_2Cl_2 solution, and the solid-state structure could be solved (Figure 1). The X-ray data are listed in Table 2, while the relevant bond angles and distances

Table 1. Comparison of the Cyclic Voltammetry Data for Selected Complexes in the dppp and dppe Series[a]

	E_{ox}(X/X$^+$)		E_{red}(X/X$^-$)	
compd	dppp	dppe	dppp	dppe
2/2′	−0.059	−0.058		
3/3′	−0.274	−0.187		
4[OTf]/4′[PF$_6$]	0.321	0.26[b]	−0.928	−0.71
5/5′	0.604	0.600		

[a] Conditions: measurements carried out in the range +1.2−1.2 V vs SCE; THF/0.1 M [Bu_4N][PF_6]; T = 20 °C; Pt electrode; 0.1 V/s; V vs SCE; $Cp_2Fe^{0/+}$ couple used as internal standard at 0.560 V vs SCE.[28] [b] From ref 1 after correction (data were reported for the $Cp_2Fe/Cp_2Fe^{0/+}$ couple used as an internal standard at 0.54 V vs SCE).

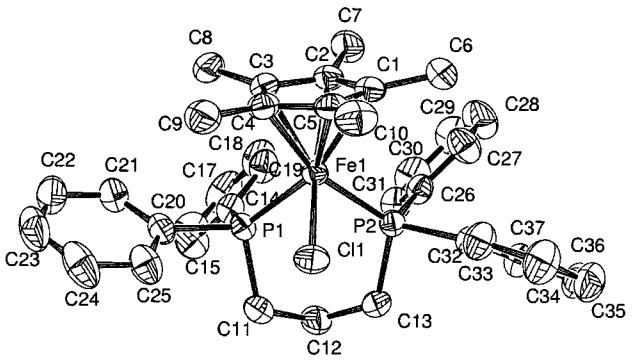

Figure 1. Molecular structure of Cp*(dppp)FeCl (**2**). Non-hydrogen atoms are represented by 50% probability thermal ellipsoids.

are given in Table 3. The complex **2** crystallizes as its homologue **2′** in the triclinic crystal system.[3] On the whole, the bond distances and angles are typical for piano-stool organoiron(II) complexes. Nevertheless, slight perturbations of the structure are induced by the presence of a third methylene group between the two phosphorus atoms. With respect to complex **2′**, the structure of compound **2** shows a weak shortening of the iron C_5-ring centroid distance of ca. 0.02 Å, an increase of ca. 0.035 Å in the Fe−P bond distances, whereas the Fe−Cl bond length remains unchanged. The major difference between these two structures deals with an increase of 7° of the P1−Fe−P2 angle in **2**. The metallacycle defined by the dppp ligand and the metal presents a chair conformation typical of six-membered cycles. Two phenyl groups and the chlorine atom occupy the axial positions, whereas the two remaining phenyl substituents and the Cp* ligand are located in the equatorial sites. This chair conformation is probably quite dominant in solution, because its inversion should

Table 2. Crystallographic Data for [Cp*(dppp)FeCl]·CH_2Cl_2 (2·CH_2Cl_2) and [Cp*(dppp)Fe][OSO_2CF_3]·$(CH_3)_2CO$ (4[OTf] ·$(CH_3)_2CO$)

		4[OTf] ·$(CH_3)_2CO$	
	2·CH_2Cl_2 293 K	293 K	110 K
mol formula	$FeP_2C_{37}H_{41}Cl·CH_2Cl_2$	$FeP_2C_{37}H_{41}(CF_3SO_3)·C_3H_6O$	
mol wt	723.86	810.64	810.64
cryst syst	triclinic	monoclinic	triclinic
space group	$P\bar{1}$	$P2_1/m$	$P\bar{1}$
cell dimens			
a (Å)	10.500(2)	11.0111(4)	10.8283(4)
b (Å)	11.830(2)	15.4655(6)	12.6358(6)
c (Å)	16.256(2)	12.7913(4)	15.2854(4)
α (deg)	79.84(1)		88.171(2)
β (deg)	72.42(1)	113.659(2)	113.659(2)
γ (deg)	66.83(2)		67.140(2)
V (Å^3)	1765.8(6)	1995.2(1)	1925.4(1)
Z	2	2	2
d_{calcd}(294 K) (g/cm^3)	1.361	1.349	1.398
abs coeff (mm^{-1})	0.771	0.564	0.585
F(000)	756	848	848
cryst dimens (mm)	0.44 × 0.37 × 0.35	0.40 × 0.35 × 0.33	0.40 × 0.35 × 0.33
diffractometer	CAD4	Nonius Kappa CCD	
radiation (Å)		Mo Kα, 0.710 73	
data collection method		$\omega/2\theta$	
measmt t_{max} (s)	60	20	20
index range (h,k,l)	0−13, −13 to +15,−19 to +20	0−14, 0−20, −16 to +14	0−14, −14 to +16, −20 to +20
θ range (deg)	54	55	55
decay of stds (25), %	0.4		
no. of rflns measd	7684	4746	25 134
no. of indep rflns	5997	3562	9176
no. of obsd data, $I > 2\sigma(I)$	5997	3562	7773
no of variables	398	238	470
R	0.042	0.086	0.092
R_w	0.113	0.252	0.259
GOF	1.019	1.183	0.986
largest diff peak and hole, (e Å^{-3})	0.61, −0.82	1.44, −1.38	3.8, −1.07

Table 3. Comparison of Key Distances (Å) and Angles (deg) for Cp*Fe(dppp)Cl (2), Cp*Fe(dppe)Cl (2′),[3] [Cp*Fe(dppp)][O_3SCF_3] (4[OTf]), and [Cp*Fe(dppe)][PF_6] (4′[PF_6])[1]

	2/2′		4[OTf][a]/4′[PF_6]	
distance/angle	dppp	dppe	dppp	dppe
Fe−P1	2.2406(8)	2.210(1)	2.2737(11)	2.126(3)
Fe−P2	2.2388(8)	2.197(1)	2.2656(11)	2.148(3)
Fe−Cp*(centroid)	1.746(3)	1.768(4)	1.802(3)	1.722(4)
Fe−X	2.3463(8)	2.346(1)	8.173[b]	
P1−Fe−P2	92.02(3)	84.98(5)	95.62(6)	86.87(8)
P1−Fe−Cl	86.80(3)	86.03(4)		
P2−Fe−Cl	88.75(3)	87.23(4)		
α[c]			178.0	175.2
θ[c]			89.1(2)	

[a] Data obtained at 110 K. [b] X = closest oxygen atom of the triflate anion. [c] See text for the definition of the angle.

produce strong 1,3-diaxial interactions between the bulky C_5Me_5 ligand and axial methylene protons.

Interestingly, the opening of the P1−Fe−P2 angle in the dppp series induces significant modification of the steric environment around the metal center. Indeed, comparison of **2** and **2′** clearly shows that the metal center and the chlorine atom are more sterically crowded in **2** than in **2′**. In particular, the two phenyl rings of the dppp in equatorial positions are very close to the chlorine. The through-space distances between their ortho carbon atoms (C25 and C33) and the chlorine atom are as short as 3.3 Å. In the complex **2′**, there is more room around chlorine, and as a result, the through-space shortest carbon−chlorine distance is 3.5 Å. Such a steric congestion could have an effect on the reactivity and the stability of the complex in the Cp*(dppp)Fe series. Moreover, we note that the distances between the chlorine atom and the axial methylene protons of the P-bound methylene groups are as short as 2.72 Å, which should give rise to through-space interactions and explain the upfield shift observed for the methylene resonance in the ^{1}H NMR spectrum.

3. Synthesis and Characterization of Cp*(dppp)FeH (3) and [Cp*(dppp)FeH][PF_6] (3$^+$). The hydride **3** was readily obtained by treatment of the chloro derivative **2** with a small excess of $LiAlH_4$ (1.2 equiv) in THF at low temperature. After in situ destruction of the alanes by successive addition of CH_3OH and CH_2Cl_2 (see Experimental Section), workup provides **3** as a pure and thermally stable orange powder in 95% yield. This reaction does not present any significant difference from that previously studied in the dppe series.[3] As already noted for **2** and **2′**, the ^{1}H and ^{13}C NMR chemical shifts observed for **3** are quite similar to those reported for its homologue of the dppe series **3′**. We note that a small upfield shift of 0.35 ppm for the hydride resonance and the ^{31}P resonance observed at δ 75.6 ppm strongly differs from that of **3′** located at δ 107.9.

Surprisingly, the replacement of the dppe by the dppp ligand produces a large decrease of the Fe−H bond stretching ($\Delta\nu$ = 69 cm^{-1}). A possible explanation for this feature, which reveals an unexpected change in the Fe−H bonding, can be found in the existence of two different conformers for **3** (**3A** and **3B**, Scheme 2), as recently proposed for **3′** on the basis of DFT calculations on the model complex CpFe(dpe)H (**3H**).[10] One of the

(10) Tilset, M.; Fjeldahl, I.; Hamon, J.-R.; Hamon, P.; Toupet, L.; Saillard, J.-Y.; Costuas, K.; Haynes, A. *J. Am. Chem. Soc.* **2001**, *123*, 9984−10000.

Scheme 2

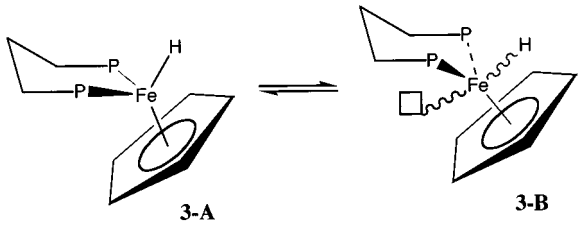

conformers, denoted HA, presents a symmetry close to C_s and adopts a three-legged piano-stool geometry comparable to those observed for halide complexes such as **2** and **2′**. In the other one, named HB, the geometry can be idealized by considering a four-legged piano-stool complex in which a vacant site occupies the fourth leg. In this conformer, the P1−Fe−P2 plane is much closer to being perpendicular to the plane of the C_5 ring of the Cp* ligand. In the case of **3H**, HB is more stable than HA by 0.10 eV and the ν_{Fe-H} stretching frequencies were computed at 1892 and 1876 cm^{-1} for HA and HB, respectively. In the case of **3**, the presence of the vacant site and its relative orientation with respect to the dppp ligand should minimize the steric interactions in the conformer **3B**. As a consequence, the conformer B could be more favored in **3** than in **3′**. The computed Fe−H bond stretching being smaller in HB than in HA,[10] it should result in a decrease of the experimental ν_{Fe-H} when the dppe is replaced by the dppp, as it is experimentally observed.

The theory also predicts that the oxidized complex $\mathbf{3H}^+$ does not exist with a C_s symmetry, but only as a four-legged piano-stool conformer.[10] Therefore, one can expect that the ν_{Fe-H} frequencies in the oxidized complexes $\mathbf{3}^+$ and $\mathbf{3'}^+$ should be closer than in the reduced forms **3** and **3′**, and to verify this assumption, $\mathbf{3}^+$ was prepared. The initial scan in the cyclic voltammogram of the complex **3** is characterized by a reversible one-electron process with a current ratio (i_p^a/i_p^c) of unity. The anodic and cathodic peak separation ($E_p^c - E_p^a$) is 0.100 V in THF with a scan rate of 0.1 V/s. The thermodynamic oxidation potential of **3** is $E° = -0.273$ V vs SCE. It appears 0.087 V more negative that its relative **3′,** which means that **3** is more easily oxidized than **3′** (Table 1).[4] Possibly, the oxidation takes place at the less stable isomer HA and the more negative redox potential observed for the oxidation of the iron hydride in the dppp series suggests that the HA conformer should be less stable in this series than in the dppe one.

Treatment of **3** with 1 equiv of $[FeCp_2][PF_6]$ in THF resulted in a rapid color change from orange to dark red. After precipitation by pentane and further recrystallization from a THF−pentane mixture, dark red thermally stable microcrystals of **3**+ were obtained in 95% yield. The complex $\mathbf{3}^+$, which shows a cyclic voltammogram identical with that of **3**, exhibits an Fe−H bond stretching at 1859 cm^{-1}. As expected, the difference in the ν_{Fe-H} frequencies between the oxidized species $\mathbf{3}^+$ and $\mathbf{3'}^+$ ($\Delta\nu = 27$ cm^{-1}) is much smaller than that between the corresponding 18-electron species.

4. Synthesis and Characterization of [Cp*(dppp)Fe][OSO_2CF_3] (4[OTf]). Reaction of **3** with 1.1 equiv of methyl triflate in diethyl ether at 20 °C caused the very slow formation of a yellow suspension. Isolated by filtration, this solid material is thermally stable, but air sensitive. Recrystallization from an acetone solution by addition of pentane afforded the 16-electron species $[Cp^*(dppp)Fe][OSO_2CF_3]$ (**4[OTf]**), isolated as the triflate salt in 82% yield. The IR spectrum of **4[OTf]** shows three well-defined absorption bands at 1273, 1159, and 1029 cm^{-1}. Bands in this range of frequencies can be observed either for triflate coordinated at a metal center or for ionic free triflate anion.[11,12] Note that these bands are also observed in the spectra of the compounds **5** and **6** (see below). More characteristic of a noncoordinated triflate anion is the absence of the sulfonyl stretching mode above 1300 cm^{-1}.[13] In contrast, such a feature was observed in the IR spectrum of the $[Cp^*(dppe)Fe(OSO_2CF_3)]$ (**4′-OTf**) complex at 1305 cm^{-1}.[12,14]

The triflate anion was definitely demonstrated to be not coordinated to the metal center by an X-ray crystallographic analysis. Monocrystals of **4[OTf]**·$(CH_3)_2CO$ were grown by slow diffusion of pentane in a concentrated acetone solution, and the crystal structure was determined at 293 and 110 K, as outlined in Table 2 and Figure 2. Key distances and angles are given in Table 3. The complex **4[OTf]**·$(CH_3)_2CO$ crystallizes in the monoclinic crystal system and in the $P2_1/m$ space group. A phase transition occurs upon cooling, and the molecule is found in the triclinic crystal system and $P\bar{1}$ space group at 110 K. On the whole, the molecule presents the same geometric characteristics in both structures. At 293 K, the triflate anion was found disordered between two symmetric positions with respect to the plane of symmetry of the complex. In contrast, the triflate anions occupy well-defined positions of the unit cell in the structure recorded at 110 K. The reversibility of the phase transition was established by a new determination of the unit cell parameters after warming up the crystal to room temperature (293 K).

The structure of **4[OTf]** strongly contrasts with that of the previously reported triflate complex $[Cp^*(dppe)Fe(OSO_2CF_3)]$ (**4′-OTf**).[1] Indeed, the complex **4[OTf]** does not present a pseudo-octahedral geometry, and the shortest iron−oxygen distance of 8.17 Å clearly shows that neither the triflate anion nor acetone is coordinated to the metal. General features, such as the formally trigonal-bipyramidal geometry (hybridization dsp^3) at the metal, are in accord with a formal 16-electron complex. The X-ray structures show a molecule close to C_{2v} symmetry with two almost equivalent phosphorus atoms. The angle α, defined by the ring centroid, the Fe atom, and the middle of the P1−P2 vector (α = 178°), and the dihedral angle θ, formed by the plane of the Cp* ligand and the plane defined by the three atoms P1, Fe, and P2 (θ = 89.1(2)°), are close to the ideal geometry. Moreover, the shortest distance between the

(11) (a) Lawrance, G. A. *Chem. Rev.* **1986**, *86*, 17−33. (b) Beck, W.; Sünkel, K. *Chem. Rev.* **1988**, *88*, 1405−1421.

(12) (a) Jonston, D. H.; Shriver, D. F. *Inorg. Chem.* **1993**, *32*, 1045−1047. (b) Schwiebert, K. E.; Stryker, J. M. *Organometallics* **1993**, *12*, 600−602.

(13) Stang, P. J.; Huang, Y.; Arif, A. M. *Organometallics* **1992**, *11*, 231−237.

(14) (a) Hamon, P.; Hamon, J.-R.; Lapinte, C. Unpublished results. (b) Blake, D. M. *J. Chem. Soc., Chem. Commun.* **1974**, 815. (c) Blosser, P. W.; Gallucci, J. C.; Wojcicki, A. *Inorg. Chem.* **1992**, *31*, 2376−2384. (d) Merrifield, J. H.; Fernandez, J. M.; Buhro, W. E.; Gladysz, J. A. *Inorg. Chem.* **1984**, *23*, 4022−4029. (e) Tolman, W. B. *Inorg. Chem.* **1991**, *30*, 4877−4880. (f) Legzdins, P.; Smith, K. M.; Rettig, S. J. *Can. J. Chem.* **2001**, *79*, 502−509.

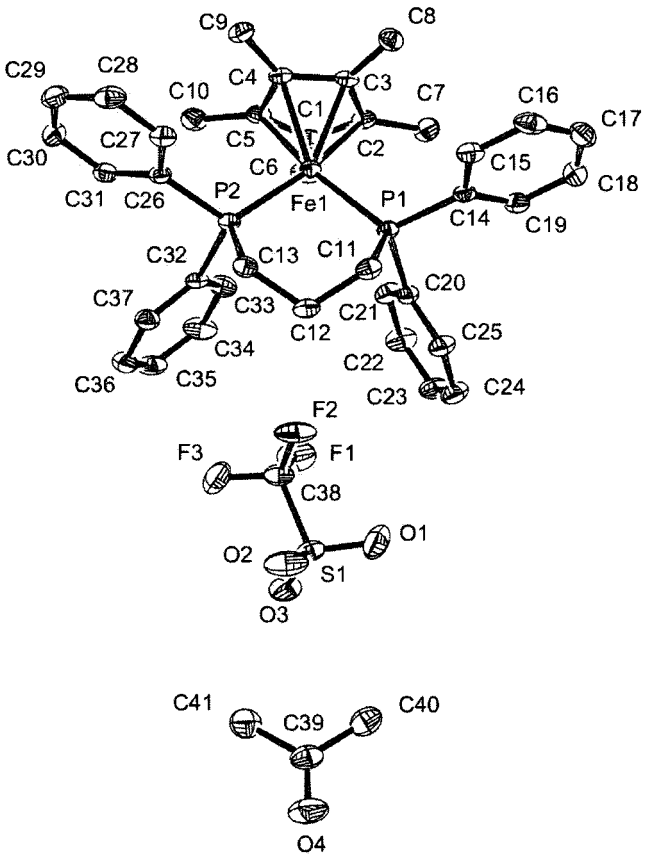

Figure 2. Molecular structure of [Cp*(dppp)Fe][SO_3CF_3]·$(CH_3)_2CO$ (**4[OTf]**) at 110 K. Non-hydrogen atoms are represented by 50% probability thermal ellipsoids.

iron site and the ortho carbon atoms of the phenyl groups of the dppp is 3.50 Å, definitely excluding an agostic interaction between the electron-deficient metal center and a C−H bond.

One can recall that crystallization of the 18-electron compound [Cp*(dppe)Fe(OSO_2CF_3)] from an acetone−pentane mixture provided the σ-acetone complex [Cp*(dppe)Fe{σ-O=C$(CH_3)_2$}][OSO_2CF_3].[8] Moreover, an X-ray crystal structure determination established the C_s symmetry of this complex and the Fe−O distance of 2.031(4) Å. Therefore, the introduction of an extra methylene fragment between the two phosphorus atoms of the dppp ligand produces a dramatic change in the coordinating properties of the iron center. This difference of behavior between the dppe and dppp series was unpredictable but should be explained by both steric and electronic considerations. The steric congestion observed around the metal in the case of complex **2** should not give enough room in the vicinity of the iron center to allow the coordination of neutral or even anionic ligand as large as acetone or triflate. Indeed, one can assume that 1,3-diaxial interactions between the atoms of the triflate group or the acetone molecule as well, and the axial hydrogen atoms of the methylene fragments should be too strong.

On the other hand, the opening of the P−Fe−P angle in the dppp series should induce significant changes in the electronic structure of the16-electron species [Cp*(dppp)Fe]$^+$ with respect to that of [Cp*(dppe)Fe]$^+$, as suggested by their different colors. Indeed, the complex **4[OTf]** is yellow, whereas the corresponding 16-electron derivative of the dppe series **4′[PF_6]** is dark red. The UV−vis spectrum of **4[OTf]** in THF displays a π−π* high-energy transition at 36 760 cm^{-1} (ϵ = 4400 M^{-1} cm^{-1}) and an absorption band centered at 29 630 cm^{-1} (ϵ = 2000 M^{-1} cm^{-1}) with a shoulder at 23 260 cm^{-1} (ϵ = 360 M^{-1} cm^{-1}) corresponding to HOMO−LUMO transitions. The spectrum of the corresponding 16-electron species in the dppe series displays much more intense transitions at 35 710 cm^{-1} (ϵ = 9200 M^{-1} cm^{-1}) and 31 496 cm^{-1} (ϵ = 5680 M^{-1} cm^{-1}) with a shoulder at 23 250 cm^{-1} (ϵ = 900 M^{-1} cm^{-1}). As a result, it appears that the increase of the P(1)−Fe−P(2) angle from 86.87(8)° in **4′[PF_6]** to 95.50(6)° in **4[OTf]** is associated with the decrease of the HOMO−LUMO gap of 1867 cm^{-1} (ca. 0.23 eV).[15] According to the theoretical approach of Saillard and Costuas, it turns out that the phosphorus participation in the HOMO and LUMO orbitals is 3% and 15%, respectively, for the pseudo-C_{2v} geometry of the [CpFe$(PH_3)_2$]$^+$ model compound.[9] Therefore, one can predict that the decrease of the HOMO−LUMO gap induced by the replacement of the dppe by the dppp ligand should be mainly due to the stabilization of the LUMO rather than an increase of the energy level of the HOMO.

The initial scan in the cyclic voltammogram of the complex **4[OTf]** displays two reversible waves in THF with the $E°$ potentials at −0.928 and 0.321 V vs SCE. The chemical reversibility at the platinum electrode is established for both redox systems by the ratio of the anodic and cathodic current of unity. The electron transfer which occurs at −0.928 V vs SCE corresponds to the one-electron reduction of **4[OTf]** and the formation of the neutral 17-electron species **4**• at the platinum electrode, whereas a one-electron oxidation process takes place at 0.321 V vs SCE with the generation of the 15-electron species **[4]**$^{2+}$ on the electrode surface. Considering the high degree of reversibility of these processes, the complexes **4**• and **[4]**$^{2+}$ should constitute accessible synthetic targets, but their preparation was not attempted in the context of this project. The comparison of the reduction potentials of **4[OTf]** and **4′[PF_6]** shows that **4[OTf]** is more difficult to oxidize ($\Delta E°$ = +0.06 V) and more difficult to reduce ($\Delta E°$ = −0.22 V) than the corresponding compound of the dppe series (see Table 1). This result could be considered as not consistent with the diminution of the HOMO−LUMO gap from **4′[PF_6]** to **4[OTf]**. However, electrochemical and spectroscopic data can only be compared with *extreme caution* when spin transition occurs. Indeed, the electron transfer between the 16-electron compound **[4]**$^+$ and the 15-electron **[4]**$^{2+}$ or the 17-electron **4**• complex should occur between species in their low-spin states, whereas the HOMO−LUMO gap was determined for **4[OTf]** in its ground state, which is the triplet state (see below). Note that according to the theoretical calculations, the singlet state possesses a somewhat pyramidalized C_s conformation, which enlarges the HOMO−LUMO gap.[9] This result suggests that the variation of the bite angle of the bis-phosphine

(15) On the basis of the facility for 16-electron ruthenium [Cp*RuP_2]$^+$ complexes to make agostic interactions, it has recently been proposed that a small P1−M−P2 angle lowers the energy level of the LUMO.[26] This could be true for compounds of C_s symmetry with a significant degree of pyramidalization but is not confirmed by our results on iron complexes with pseudo-C_{2v} symmetry.

Table 4. ^{57}Fe Mössbauer Fitting Parameters at 80 K for 4[OTf][a]

T (K)	IS (mm/s)	QS (mm/s)	Γ (mm/s)
80	0.553	1.752	0.130
100	0.547	1.743	0.123
150	0.531	1.717	0.121
200	0.515	1.692	0.120
250	0.502	1.631	0.148
300	0.490	1.600	0.156
350	0.480	1.566	0.179

[a] The area percentage in all cases is 100%.

could have opposite effects on the HOMO−LUMO gap of the singlet and triplet states.[16]

On the other hand, DFT calculations carried out on the real compound [Cp*(dppe)Fe]$^+$ (**4′**) allowed the determination of the optimized geometries of the singlet ($S = 0$) and the triplet states ($S = 1$).[9] They mainly differ from their α angle, which are 162 and 177° for the singlet and the triplet states, respectively. The triplet was also found to be more stable than the singlet by 0.12 eV. In agreement with its pseudo-C_{2v} symmetry, the complex **4[OTf]** was expected to be paramagnetic. This was confirmed by the determination of its magnetic susceptibility at 293 K by the Evans method.[17] In an acetone solution, the complex **4[OTf]** exhibits the magnetic moment $\mu_{eff} = 2.93\ \mu_B$, fully compatible with the presence of two unpaired electrons in the ground state. In accord with its paramagnetic behavior, any resonance cannot be observed in the ^{31}P and ^{13}C NMR spectra of **4[OTf]**.[7,18] However, a unique and sharp signal was observed in the ^{19}F spectrum for the triflate anion at δ −73.7 ppm. The presence of the unpaired electrons affects the line width and the chemical shifts of the proton resonances, which were observed in the ^{1}H spectrum in the range 78 to −11 ppm. On the basis of the relative intensity of the peaks, the β- and α-methylene protons and the Cp* resonances were assigned to signals at δ 77.23 ($w_{1/2} = 105$ Hz), 47.14 ($w_{1/2} = 105$ Hz), and 44.85 ($w_{1/2} = 85$ Hz), respectively.

The zero-field Mössbauer spectra of a powdered sample of **4[OTf]**, run between 80 and 350 K, show a unique doublet without any traces of decomposition even after 48 h at 350 K. The values of the isomer shift (IS) range from 0.553 to 0.480 mm/s and decrease with temperature (Table 4). In agreement with the high-spin configuration of the 16-electron iron(II) complex, the isomer shifts are much larger than those found for low-spin iron(II) derivatives.[19,20] The IS values decrease almost linearly with temperature. However, careful examination of the data revealed a break in the linear relationship between IS and *T*. Indeed, in the ranges 80−200 and 200−350 K, IS decreases as a linear function of the temperature ($R \geq 0.999$) with a visible break in the slope around 200 K (Figure 3). Note that the variation of the slope is quite weak, indicating that the phase transition is not associated with a spin transition.

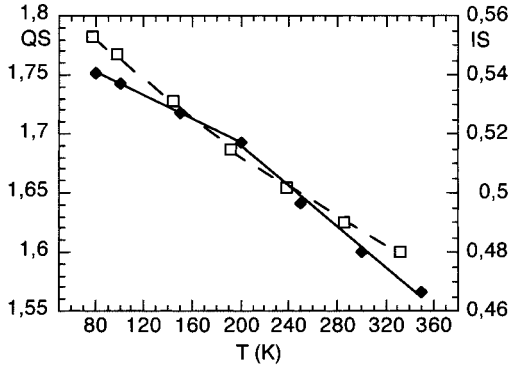

Figure 3. Temperature dependence of the ^{57}Fe parameters IS (open squares) and QS (dark squares) for the complex **4[OTf]**.

Mössbauer quadrupole splittings (QS) are quite sensitive to the nature of the bonding between the metal and the coordinated ligand.[21] The QS values determined for **4[OTf]** are significantly smaller than the values usually observed for 18-electron complexes (Table 4). Moreover, the QS value continuously decreases with temperature in the range 80−350 K. As noted for the variation of the IS, a break is also observed around 200 K in the temperature dependence of QS. As Mössbauer parameters are also sensitive to symmetry, one can assume that the phase transition revealed by the X-ray analyses at 293 and 110 K should occur at a temperature close to 200 K.[19] The reversibility of this transformation has been established by running the measurements alternatively above and below 200 K.

5. Basic Reactivity of [Cp*(dppp)Fe][OSO$_2$CF$_3$] (4[OTf]). Despite its exceptional robust character, the 16-electron complex **4[OTf]** presents a strong Lewis acid character. In particular, it gives adducts with small molecules as well as its homologue **4′[PF$_6$]**. The reaction of **4[OTf]** with H_2O reversibly provides an adduct which is thought to be [Cp*(dppp)Fe(OH_2)][O_3SCF_3]. However, the aqua complex was not isolated. Its formation was followed by ^{1}H NMR by progressive addition of H_2O to a solution of **4[OTf]** in $CD_3C(O)CD_3$. As the number of equivalents of water increases, the chemical shifts of the protons of the molecule move toward the positions expected for a diamagnetic compound. For example, the resonance attributed to the Cp* ligand moves from δ 45.1 (0 equiv of H_2O) to δ 11.2 (50 equiv of H_2O). Our data suggest that the reversible decoordination of H_2O should be an easier process than its coordination. We have also found that the removal of the solvents under vacuum provides a pure sample of **4[OTf]**.

In the presence of CH_2Cl_2, **4[OTf]** reacts to give the iron(III) derivative [Cp*(dppp)FeCl][O_3SCF_3], identified by CV and comparison with an authentic sample of its iron(II) relative **2**. However, in a mixture of CH_2Cl_2/CH_3CN (2:3 v/v), the reaction with the nitrile is much faster that the reaction with CH_2Cl_2 and the complex [Cp*(dppp)Fe($NCCH_3$)][O_3SCF_3] (**5**) is isolated as a pure compound in 95% yield. As depicted in Scheme 1, the

(16) Considering the very large distance determined between the organometallic cation and its counteranion in the solid state for **4[OTf]**, charge-transfer interactions between ion pairs seem to be highly improbable in THF. Moreover, we found that the presence of 0.5−100 equiv of [NBu_4][PF_6] does not modify the UV−vis spectrum of **4[OTf]**.

(17) (a) Bertini, I.; Luchinat, C. *NMR of Paramagnetic Molecules in Biological Systems*; Benjamin/Cummings: Menlo Park, CA, 1986. (b) Sur, S. K. *J. Magn. Reson.* **1989**, *82*, 169−173.

(18) Fettinger, J. C.; Keogh, D. W.; Poli, R. *J. Am. Chem. Soc.* **1996**, *118*, 3617−3625.

(19) Gütlich, P.; Link, R.; Trautwein, A. *Mössbauer Spectroscopy and Transition Metal Chemistry*; Springer-Verlag: Berlin, 1978; Vol. 3.

(20) Guillaume, V.; Mahias, V.; Mari, V.; Lapinte, C. *Organometallics* **2000**, *19*, 1422−1426.

(21) Guillaume, V.; Thominot, P.; Coat, F.; Mari, A.; Lapinte, C. *J. Organomet. Chem.* **1998**, *565*, 75−80.

complex **4[OTf]** also reacts with carbon monoxide to yield [Cp*(dppp)Fe(CO)][O3SCF3] (**6**) quantitatively. The properties of the complexes **5** and **6** are very similar to those of the corresponding compounds **5′** and **6′** of the dppe series. In particular, the potentials for the oxidation of **5** and **5′** are identical. We only note that the vibration of the CO ligand increases from 1932 to 1945 cm^{-1} when the dppp is replaced by the dppe chelate,[22] which suggests that the Lewis acid $[Cp^*(dppp)Fe]^+$ would be slightly stronger than $[Cp^*(dppe)Fe]^+$.

6. Conclusion

Cationic 16-electron complexes of iron or ruthenium have often been postulated as intermediates in many reactions involving 18-electron complexes of the type $[(C_5R_5)M(P_2)L]^+$ (M = Fe, Ru; L = neutral 2-electron donor ligands), but so far they have proven to be elusive to isolation and characterization. Very recently remarkably stable cationic 16-electron complexes of the types $[(C_5R_5)Ru(N-N)]^+[BAr'_4]^-$ (R = Me, N−N = TMEDA,[23] $Me_2NCH_2CH_2NBu_2$;[24] R = H, N−N = TMEDA;[25] Ar′ = 3,5-$C_6H_3(CF_3)_2$) and $[Cp^*Ru(P_2)]^+[BAr'_4]^-$ (P_2 = dippe, $(PMe^iPr_2)_2$)[26] and the neutral homologue[27] were isolated and unambiguously characterized. Interestingly, it was nicely shown that the cation $[Cp^*Ru(dippe)]^+$ is stabilized by an agostic interaction with one of the hydrogen atoms of an isopropyl group, whereas such an interaction is absent in the cation $[Cp^*Ru(PMe^iPr_2)_2]^+$. In the Cp-iron chemistry, examples of 16-electron cations are mainly elusive. To the best of our knowledge, the complexes $[Cp^*Fe(dppe)]^+[PF_6]^-$ and $[Cp^*Fe(dppp)]^+[OTf]^-$ constitute the unique examples known to date. Moreover, considering the ability of the triflate anion to bind coordinatively unsaturated transition-metal complexes, the 16-electron species $[Cp^*Fe(dppp)]^+$ can be regarded as one of the less coordinating transition metal Lewis acids. This work also emphasizes that playing with the bite angle of the bis-phosphine ligand in the $Cp^*Fe(P)_2$ series allows a fine-tuning of the HOMO−LUMO gap.

Experimental Section

General Data. All the manipulations and workup procedures of air-sensitive compounds were carried out under inert atmosphere in a JACOMEX drybox filled with argon, or using standard Schlenk techniques. Reagent grade tetrahydrofuran (THF), pentane, and diethyl ether were predried and then distilled under argon from sodium benzophenone ketyl prior to use. Acetonitrile and dichloromethane were distilled under argon from P_2O_5, and acetone was distilled under argon from B_2O_3. All glassware was oven-dried prior to use. Infrared spectra were obtained as KBr disks on a Bruker IFS28 FT-IR spectrometer (400−4000 cm^{-1}). NMR spectra were acquired at 297 K on multinuclear Bruker DPX 200 (200 MHz) or AM 300 WB (300 MHz) instruments. Chemical shifts are given in parts per million (ppm) relative to tetramethylsilane (TMS) for ^1H and ^{13}C NMR spectra, external 85% H_3PO_4 for ^{31}P NMR spectra, and external $CFCl_3$ for ^{19}F spectra. Cyclic voltammograms were recorded using an EG&G-PAR Model 263 potentiostat/galvanostat. The working electrode was a Pt-disk electrode (d = 1.0 mm), the counter electrode was a Pt wire, and a saturated calomel electrode (SCE) was used as a reference electrode. The $Cp_2Fe^{0/+}$ couple was used as an internal calibrant for the potential measurements.[28] Mössbauer spectra were recorded with a 2.5×10^{-2} Ci (9.25×10^8 Bq) ^{57}Co source using a symmetric triangular sweep mode.[29] Computer fitting of the Mössbauer data to Lorentzian line shapes were carried out with a previously reported computer program.[30] The isomer shift values are reported relative to iron foil at 298 K and were not corrected for the temperature-dependent second-order Doppler shift. Magnetic susceptibility measurements were conducted in solution according to the Evans method.[17] Elemental analyses were performed at the Center for Microanalyses of the CNRS at Vernaison, France. Reagents were obtained as follows: pentamethylcyclopentadiene (Cp^*H)[31] and dppp[32] were prepared according to published procedures, and other chemicals were purchased from commercial sources and used as received. $FeCl_2$(dppp) was prepared by following a procedure similar to that used to synthesize $FeCl_2$(dppe),[33] by refluxing overnight an equimolar amount of $FeCl_2(THF)_{1.5}$ and dppp in THF. At 20 °C, the white precipitate is filtered off, washed with diethyl ether, and dried under vacuum.

Cp*(dppp)FeCl (2). A Schlenk tube was charged with $FeCl_2$(dppp) (**1**; 2.15 g, 4.00 mmol), Cp*Li (0.566 g, 4.00 mmol), and a magnetic bar. Then 20 mL of THF was added under argon. The reaction mixture, which was stirred overnight (16 h) at 20 °C, gradually turned dark. The solvent was removed under vacuum and the residue extracted with 100 mL of diethyl ether. Crystallization from a CH_2Cl_2/pentane mixture provided 2.18 g (85% yield) of Cp*Fe(dppp)Cl (**2**) as air-stable black crystals. Anal. Calcd for $C_{37}H_{41}ClFeP_2 \cdot CH_2Cl_2$: C, 63.05; H, 5.99. Found: C, 62.38; H, 6.15. ^1H NMR (300 MHz, C_6D_6): δ 8.25 (s, 4 H, Ph), 7.48−7.11 (m, 16 H, Ph), 2.54 (m, 2 H, CH_2), 1.92 (m, 2 H, CH_2), 1.35 (s, 17 H, CH_2 and Cp*). ^{31}P NMR (121 MHz, C_6D_6): δ 50.9 (s, dppp). CV (THF, 20 °C, 0.1 M $^nBu_4NPF_6$, v = 0.1 V/s): $E°$ = −0.059 V (ΔE_p = 0.166 V, i_p^a/i_p^c = 1.0). X-ray-quality crystals of $Cp^*Fe(dppp)Cl \cdot CH_2Cl_2$ were grown by slow diffusion of pentane into a saturated CH_2Cl_2 solution of the compound prepared above.

Cp*(dppp)FeH (3). At −80 °C, to a 50 mL dark green THF solution of **2** (1.12 g, 1.78 mmol) was added 0.84 g (2.20 mmol) of $LiAlH_4$. The color of the reaction medium turned progressively orange, while the temperature was raised overnight (16 h) to 20 °C. The reaction medium was then cooled to −80 °C, and 1 mL of MeOH was added dropwise. At room temperature, 0.5 mL of CH_2Cl_2 was added and the stirring was continued for an additional 5 min. The solvents were removed under vacuum, and the solid residue was extracted with 2 × 20 mL portions of diethyl ether. The ethereal solution was taken to dryness to give 1.03 g (95% yield) of an air and thermally stable orange powder of Cp*Fe(dppp)H. Anal. Calcd for $C_{37}H_{42}FeP_2$: C, 73.51; H, 7.00; P, 10.25. Found: C, 73.10; H, 7.05; P, 10.95. IR (KBr, cm^{-1}): 1800 (ν_{Fe-H}). ^1H NMR (200 MHz, C_6D_6): δ 7.90−7.84 (m, 8 H, Ph), 7.30−7.25 (m, 12 H, Ph), 2.39 (m, 2 H, CH_2), 1.70 (m, 4 H, CH_2), 1.59 (s, 15 H, Cp*), −16.42 (t, 1 H, J_{PH} = 70 Hz, Fe−H). ^{13}C NMR (50 MHz, C_6D_6): δ 143.4−

(22) While the value of ν_{CO} has been previously reported,[41] we have measured it again with a more accurate FT-IR spectrometer.
(23) Gemel, C.; Mereiter, K.; Schmid, R.; Kirchner, K. *Organometallics* **1997**, *16*, 5601−5603.
(24) Gemel, C.; Sapunov, V. N.; Mereiter, K.; Ferencic, M.; Schmid, R.; Kirchner, K. *Inorg. Chim. Acta* **1999**, *286*, 114−120.
(25) Gemel, C.; Huffman, J. C.; Caulton, K. G.; Mauthner, K.; Kirchner, K. *J. Organomet. Chem.* **2000**, *593−594*, 342−353.
(26) Tenorio, M. J.; Mereiter, K.; Puerta, M. C.; Valerga, P. *J. Am. Chem. Soc.* **2000**, *122*, 11230−11231.
(27) Yamaguchi, Y.; Nagashima, H. *Organometallics* **2000**, *19*, 725−727.
(28) Connelly, N. G.; Geiger, W. E. *Chem. Rev.* **1996**, *96*, 877−910.
(29) Varret, F.; Mariot, J.-P.; Hamon, J.-R.; Astruc, D. *Hyperfine Interact.* **1988**, *39*, 67−81.
(30) (a) Boinnard, D.; Bousseksou, A.; Dworkin, A.; Savariault, J.-M.; Varret, F.; Tuchagues, J.-P. *Inorg. Chem.* **1994**, *33*, 271−281. (b) Varret, F. In *International Conference on Mössbauer Effect Applications*; Jaipur, India, 1981; Indian Science Academy: New Delhi, 1982.
(31) Kohl, F. X.; Jutzi, P. *J. Organomet. Chem.* **1983**, *243*, 119−121.
(32) Hoffmann, R. *Angew. Chem., Int. Ed. Engl.* **1982**, *21*, 711−800.
(33) Mays, M. J.; Sears, P. L. *J. Chem. Soc., Dalton Trans.* **1973**, 1873−1875.

125.0 (m, Ph), 85.3 (s, C_5Me_5), 37.4 (tt, CH_2, $^1J_{CH}$ = 120 Hz), 31.2 (tm, CH_2, $^1J_{CH}$ = 139 Hz), 20.7 (t, CH_2, $^1J_{CH}$ = 129 Hz), 11.6 (q, C_5Me_5, $^1J_{CH}$ = 126 Hz). ^{31}P NMR (81 MHz, C_6D_6): δ 75.6 (dd, J_{HP} = 70 Hz, J_{PP} = 29 Hz, dppp). CV (THF, 20 °C, 0.1 M ^{n}Bu$_4$NPF$_6$, ν = 0.1 V/s): $E°$ = −0.274 V (ΔE_p = 0.100 V, i_p^a/i_p^c = 1.0).

[Cp*Fe(dppp)H][PF$_6$] (3$^+$). At 20 °C, 0.604 g (1.0 mmol) of **3** was dissolved in 20 mL of THF, and 0.298 g (0.9 mmol) of ferrocenium hexafluorophosphate was added to this orange solution. The reaction medium was stirred for 1 h, and the volume of the solution was reduced to 3 mL. Addition of 50 mL of pentane caused the precipitation of a red powder. After filtration the solid was washed with 3 × 50 mL of diethyl ether, and crystallization from a THF/pentane mixture provided 0.646 g (95% yield based on Cp_2FePF_6) of [Cp*Fe(dppp)H][PF$_6$] isolated as air-sensitive dark red crystals. Anal. Calcd for $C_{37}H_{42}FeF_6P_3$: C, 59.29; H, 5.65; P, 12.40. Found: C, 59.78; H, 5.55; P, 12.92. IR (KBr, cm^{-1}): 1859 (ν_{Fe-H}).

[Cp*(dppp)Fe][CF$_3$SO$_3$] (4[OTf]). To a 30 mL orange solution of **3** (0.18 g, 0.30 mmol) in diethyl ether was added 37 μL (0.33 mmol) of MeOTf. The reaction mixture was stirred for 12 h at 20 °C, and a yellow suspension was formed very slowly. The suspension was filtered off and washed with 2 × 10 mL of pentane. The solid residue was then dissolved in 10 mL of acetone and precipitated by addition of 100 mL of cold pentane (−80 °C). The solid material was filtered, washed with pentane, and dried under vacuum. The compound **4[OTf]** was recovered as an air- and moisture-sensitive yellow powder (0.187 g, 82%). Anal. Calcd for $C_{38}H_{41}F_3FeO_3P_2S·0.5(CH_3)_2CO$: C, 60.70, H, 5.67, P, 7.93. Found: C, 61.18, H, 5.67, P, 7.20. IR (KBr, cm^{-1}): 3057, 2984, 2913, 2858, 1484, 1436 (dppp), 1273 (OTf), 1159 (OTf), 1029 (OTf). ^{1}H NMR (200 MHz, CD_3COCD_3): δ 77.23 (s, 2 H, CH_2, $w_{1/2}$ = 105 Hz), 47.14 (s, 4 H, CH_2, $w_{1/2}$ = 105 Hz), 44.85 (s, 15 H, Cp*, $w_{1/2}$ = 85 Hz), 7.77 (Ph, $w_{1/2}$ = 25 Hz), 3.96 (Ph, $w_{1/2}$ = 26 Hz), −10,96 (Ph, $w_{1/2}$ = 158 Hz). ^{19}F NMR (188 MHz, CD_3COCD_3): δ −73.7 (s, CF_3). μ_{eff} (CD_3COCD_3, 297 K): 2.93 μ_B. CV (THF, 20 °C, 0.1 M ^{n}Bu$_4$NPF$_6$, ν = 0.1 V/s): $E°_1$= +0.321 V (ΔE_p = 0.164 V, i_p^a/i_p^c = 1.0); $E°_2$= −0.928 V (ΔE_p = 0.144 V, i_p^a/i_p^c = 1.0). X-ray-quality crystals of [Cp*Fe(dppp)][CF$_3$SO$_3$]·Me$_2$CO were grown by slow diffusion of pentane into a saturated acetone solution of the compound prepared above.

[Cp*Fe(dppp)(NCMe)][CF$_3$SO$_3$] (5). At room temperature, 0.030 g (0.040 mmol) of **4[OTf]** was dissolved in 2 mL of CH_2Cl_2, and 3 mL (0.050 mmol) of CH_3CN was added with a syringe. The solution was stirred overnight while the color changed from yellow to red-orange. The solvents were removed under reduced pressure. The solid residue was washed with 2 × 10 mL of pentane and dried under vacuum to give 0.030 g (95%) of **5** as an air- and moisture-stable red-orange powder. Anal. Calcd for $C_{40}H_{44}F_3FeNO_3P_2S$: C, 60.54; H, 5.59; P, 7.81. Found: C, 61.21; H, 5.80; P, 8.13. IR (KBr, cm^{-1}): 2240 (C−N), 1485, 1437 (dppp), 1275 (s, OTf), 1156 (s, OTf), 1029 (OTf). ^{1}H NMR (200 MHz, CD_3COCD_3): δ 8.02−7.49 (m, 20 H, Ph), 2.99 (s, 3 H, CH_3), 2.49 (m, 2 H, CH_2), 2.12 (m, 4 H, CH_2), 1.27 (s, 15 H, C_5Me_5). ^{13}C NMR (50 MHz, CD_3COCD_3): δ 135.1 (s, N*C*Me), 134.8−128.5 (m, Ph), 87.7 (s, C_5Me_5), 29.8 (m, CH_2), 20.3 (m, CH_2), 9.4 (q, $^1J_{CH}$ = 128 Hz, C_5Me_5), 5.6 (q, $^1J_{CH}$ = 138 Hz, *C*H$_3$CN). ^{31}P NMR (81 MHz, CD_3COCD_3): δ 52.5 (s, dppp). CV (THF, 20 °C, 0.1 M ^{n}Bu$_4$NPF$_6$, ν = 0.1 V/s): $E°$ = +0.604 V (ΔE_p = 0.088 V, i_p^a/i_p^c = 1.0).

[Cp*Fe(dppp)(CO)][CF$_3$SO$_3$] (6). At room temperature under argon, 0.075 g (0.10 mmol) of **4[OTf]** was dissolved in 5 mL of THF to provide a clear yellow solution. The Schlenk tube was then evacuated and filled with CO (1 atm) and the stirring was maintained for 1 h, while the color of the solution progressively lightened. The solvent was removed under reduced pressure. The solid residue was washed with 3 × 20 mL of pentane, and dried under vacuum, to give 0.076 g (97%) of an air-stable lemon yellow powder of **6**. IR (KBr, cm^{-1}): 1932 (ν_{CO}), 1274 (OTf), 1155 (OTf), 1029 (OTf). ^{1}H NMR (200 MHz, CD_3COCD_3): δ 7.72−7.59 (m, 20 H, Ph), 2.80 (m, 2 H, CH_2), 2.21 (m, 4 H, CH_2), 1.84 (s, 15 H, C_5Me_5). ^{13}C NMR (50 MHz, CD_3COCD_3): δ 221,2 (t, CO, $^2J_{PC}$ = 25 Hz), 135.1−129.1 (m, Ph), 96.8 (s, C_5Me_5), 32.5 (tm, CH_2, $^1J_{CH}$ = 139 Hz), 20.6 (t, CH_2, $^1J_{CH}$ = 129 Hz), 9.7 (q, $^1J_{CH}$ = 129 Hz, C_5Me_5).^{31}P NMR (CD_3COCD_3): δ 49.9 (d, J_{PP} = 31 Hz, dppp).

Crystallography. Data were collected on crystals of **2**·CH_2Cl_2 and **4[OTf]**·$(CH_3)_2CO$ as summarized in Table 2.[34] Cell constants and an orientation matrix of **2**·CH_2Cl_2 were obtained from a least-squares refinement using 25 high-θ reflections. After Lorentz and polarization corrections[35] and absorption corrections (φ scans), the structure was solved with SIR-97,[37] which revealed the non-hydrogen atoms and the CH_2Cl_2 solvate. After anisotropic refinements, a Fourier difference map revealed many hydrogen atoms. Cell parameters of **4**·[OTf] are obtained with Denzo and Scalepack[37] with 10 frames (psi rotation: 1° per frame). The data collection[34b] ($2\theta_{max}$ = 60°, 163 frames via 1.9° omega rotation and 38 s per frame) gives 25 134 integrated reflections. The data reduction with Denzo and Scalepack[37] leads to 9176 independent reflections (7773 with $I > 2.0\sigma(I)$). The structure was solved with SIR-97,[37] which revealed all the non-hydrogen atoms of the structure. The whole structure was next refined by SHELX-97[38] by full matrix least-squares techniques (use of F^2 magnitude; x, y, z, β_{ij} for Fe, P, N, O, and C atoms and x, y, and z in the riding mode for H atoms; w(calcd) = $1/[\sigma^2(F_o^2) + (0.0911P)^2 + 4.5203P]$, where $P = (F_o^2 + 2F_c^2)/3$). Atomic scattering factors were taken from the literature.[39] Ortep views were generated with PLATON-98.[36] All calculations were performed on a Pentium NT Server computer.

Acknowledgment. We gratefully acknowledge Drs K. Costuas, J.-F. Halet, and J.-Y. Saillard for many interactive and stimulating discussions.

Supporting Information Available: Tables of crystal data, atomic coordinates, bond lengths and angles, and anisotropic thermal parameters for **2**·CH_2Cl_2 and **4[OTf]**·$(CH_3)_2CO$. This material is available free of charge via the Internet at http://pubs.acs.org.

OM0108245

(34) (a) Fair, C. K. *MOLEN*; An Interactive System for Crystal Structure Analysis; Enraf-Nonius: Delft, The Netherlands, 1990. (b) *Nonius KappaCCD Software*; Nonius BV: Delft, The Netherlands, 1999.

(35) Spek, A. L. *HELENA*; Program for the handling of CAD-4 Diffractometer Output SHELX(S/L); Utrecht University: Utrecht, The Netherlands, 1997.

(36) Altomare, M. C.; Burla, M.; Camalli, G.; Cascarano, C.; Giacovazzo, A.; Guagliardi, A. G. G.; Moliterni, G.; Polidori, R.; Spagna, R. Sir97: a new tool for crystal structure determination and refinement. *J. Appl. Crystallogr.* **1998**, *31*, 74−77.

(37) Otwinowski, Z.; Minor, W. Processing of X-ray Diffraction Data Collected In Oscillation Mode. In *Methods in Enzymology*, Vol. 276, Macromolecular Crystallography, Part A; Carter, C. W., Sweet, R. M., Eds.; Academic Press: London, 1997; p 307.

(38) Sheldrick, G. M. *SHELX97*; Program for the Refinement of Crystal Structures; University of Göttingen: Göttingen, Germany, 1997.

(39) *International Tables for X-ray Crystallography*; Wilson, A. J. C., Ed.; Kluwer Academic Publishers: Dordrecht, 1992; Vol. C.

(40) Spek, A. L. *PLATON-98*; A Multipurpose Crystallographic Tool; Utrecht University: Utrecht, The Netherlands, 1998.

(41) Catheline, D.; Astruc, D. *Organometallics* **1984**, *3*, 1094−1100.